Construction and Building Materials 50 (2014) 1–12

Contents lists available at ScienceDirect

Construction and Building Materials

journal homepage: www.elsevier.com/locate/conbuildmat

Activation of liberated concrete fines and their application in mortars

M.V.A. Florea *, Z. Ning, H.J.H. Brouwers

Department of the Built Environment, Unit Building Physics and Services, Eindhoven University of Technology, P.O. Box 513, 5600MB Eindhoven, The Netherlands

HIGHLIGHTS

- Recycled concrete fines (RCF) are activated through a thermal treatment method.
- RCF can be used in mortar samples up to 20% cement replacement.
- 800 °C-treated RCF had mechanical performances equivalent to fly ash.
- Thermally treated RCF showed an activation effect on ground blast furnace slag.
- A calcium silicate phase is formed during the treatment of RCF at 800 °C.

ARTICLE INFO

Article history:
Received 7 April 2013
Received in revised form 8 September 2013
Accepted 12 September 2013
Available online 3 October 2013

Keywords:
Recycled concrete
Fines
Activation
Slag
Cement replacement
Mortar
Thermal treatment

ABSTRACT

Cement is the most energy-consuming component of concrete, leading to a high CO_2 release during its fabrication. Therefore, a reduction of the cement amount used in concrete mixtures would be beneficial from an environmental point of view. One way to do this is by replacing cement with a suitable material; in this research, recycled concrete fines obtained from crushed concrete (RCF) is used to replace part of the cement in new mortar recipes. RCF subjected to various thermal treatments were used to replace part of the cement in the standard mortar samples containing either OPC or slag- or fly-ash blended cements. Both untreated and thermally-treated RCF were characterized in terms of density, PSD, composition (XRF and XRD, as well as SEM), calorimetric behavior and mechanical strength when added into mortars. Mortar samples were tested and the results show that RCFs can be a beneficial addition, especially in the case of blended cements.

1. Introduction

The European Cement Association [1] reported that 3.6 billion tons of cement were produced worldwide in 2011. Cement production figures amount to about 8–12% of concrete production, which leads to between 28 and 43 billion tons concrete produced in 2011. The production of cement has been linked to a high CO_2 emission, this industry being estimated to generate ~7% of all liberated CO_2 [2]. Besides this, the cement industry is known to consume both energy and natural resources (water and mineral raw materials) in large amounts. The replacement of concrete ingredients – either cement or aggregates – can lead to a reduction in both the generation of CO_2 and the use of natural resources. An increasing source for both these types of replacement could be concrete and demolition waste, cleaned and treated in order to be used again in the building industry.

1.1. Construction and demolition waste

The World Business Council for Sustainable Development has quantified [3] the C&D waste generation and recovery of a number of countries. The total C&D waste generated in 2011 ranged between 14 Mt in Australia to 201 Mt in Germany and 309 Mt in France. These large amounts of construction and demolition waste, if not treated properly in order to be reused, need to be landfilled as normal waste.

The main reasons for the increase of the volume of C&D waste are old structures that have overcome their use expectancy and need to be demolished, new requirements and necessities leading to the demolition of otherwise still viable structures and destructive natural phenomena like earthquakes and storms [4].

The main re-use purpose for C&D waste is road-base material. However, an important application is also their use as aggregates in new concrete mixes. When comparing recycled aggregates to new aggregates or other building materials, a number of factors need to be taken into account [5]. A first factor is the land use impact – the use of recycled aggregates means that less waste goes to

* Corresponding author. Tel.: +31 402474687; fax: +31 402438595.
E-mail address: m.v.a.florea@tue.nl (M.V.A. Florea).

0950-0618/$ - see front matter © 2013 Elsevier Ltd. All rights reserved.
http://dx.doi.org/10.1016/j.conbuildmat.2013.09.012

landfill, while also reducing the need of producing new aggregates. Another important factor is the transportation cost (including fuel use and CO_2 emissions), which can be much lower than in the case of new aggregates, if the C&D waste is located close to the construction site. New aggregates are usually transported from distant quarries to the construction site. Also to be mentioned are the useful life expectations – using recycled aggregates means that the concrete itself has a longer period of use than the structure it was initially part of.

1.2. The use of C&D waste as aggregates in new concrete

In the European Union, it is estimated that the construction and demolition rubble amounts to 500 kg per capita annually [5]. High recycling rates are achieved in countries like The Netherlands, Japan, Belgium and Germany. The Netherlands had in 2011 a very high rate of C&D waste recovery, of approximately 95% of the generated 26 Mt [6]. In the US, the recycled aggregates can be divided by use in pavements (10–15%), other road construction and maintenance work (20–30%) and structural concrete (60–70%). Recycled aggregates are produced by natural aggregates producers (50%), contractors (36%) and debris recycling centers (14%) [7]. In Japan, the concrete recycling ratio reached 98% in 2003, from 65% in 1995, the most common application being as sub-base material in road construction [4]. Tam [4] analyzed the situation of C&D waste recycling in Australia. It was found that concrete constitutes 81% of total C&DW. The concrete recycling rate in Australia is about 40%, where it is mainly used for low-grade applications. The amount of C&D waste in China has reached 30–40% of the whole amount of municipal solid wastes (MSW), with waste concrete occupying a large percentage (around one third), according to Li [8]. The main identified sources for waste concrete in China are demolished concrete structures and elements, rejected structural precast members, laboratory-cast concrete specimens and airport pavements.

1.3. The use of C&D waste fine fractions in new concrete

The possibility of using recycled concrete fines to replace a part of the cement in the concrete recipes is investigated in the present study.

Through a thermal treatment, hydrated cement paste can be dehydrated. Shui et al. [9] researched dehydrated cement paste (DCP) in depth, concluding that hardened cement paste treated at 500 °C is mainly composed of dehydrated C–S–H, CaO, partially CH and non-crystalline dehydrated phases. Upon contact of the dehydrated paste with water, the initial hydration products such as the C–S–H gel, ettringite and CH are recovered.

2. The dehydration and rehydration of hardened cement paste

2.1. The effects of thermal treatment on recycled concrete particles

During high temperature exposure of hardened cement paste (HCP), a sequence of physical and chemical processes takes place [9]. The main phenomenon is the evaporation of water from the HCP – both physically and chemically bound. Through this process, first the pore water, and then a part of the water retained by the hydration products is lost. Above 120 °C, structural changes begin to take place, including the dehydration of $Ca(OH)_2$ (CH) around 450 °C and decarbonation of $CaCO_3$ ($C\bar{C}$) around 750 °C. The dehydration process of HCP is completed at the temperature of 800 °C or above. Thus, a dehydrated cement paste (DCP) at a certain temperature will consist of partially or totally dehydrated products, hydration products that might not have been affected by the thermal treatment, and unhydrated cement. Castello et al. [10] report the decomposition of ettringite at a temperature as low as 90 °C, even lower than the temperature at which the free water is eliminated (105°). Alonso and Fernandes [11] concluded that ettringite became dehydrated abruptly after the temperature of 100 °C.

The C–S–H gel is reported to start dehydration between the temperatures of 200 °C and 400 °C [10]. Handoo et al. [12] found by employing a scanning electron microscopy analysis that the morphological changes of the C–S–H gel take place mainly at a temperature higher than 600 °C. Alonso and Fernandes [11] concluded that the C–S–H gel starts to dehydrate slightly as early as 100–200 °C, dehydrating gradually with the increase of temperature. They observed that from 600 °C to 750 °C, the solid phases in DCP contain mainly dehydrated C–S–H, CaO, anhydrous phases and dehydrated ettringite.

Tayyib [13] reported that portlandite decomposes at a relatively low temperature of about 400 °C. However, Castello et al. [10] concluded that portlandite dehydrates between 530 °C and 560 °C. Table 1 gives an overview of the main transformations in a HCP with their respective temperatures.

All these decompositions take place with a mass loss, comprising usually of water or carbon dioxide. However, one of the processes that take place during the dehydration of HCP is a phase transformation, which takes place without mass loss, but with a change in the structure. This is the transformation of crystalline silica from its α to the β form. Therefore, at around 580 °C, the sand structure breaks down, but does not affect the mass of the sample (Table 1).

2.2. Rehydration of dehydrated cement pastes

It is found by Shui et al. [9,14,15] that dehydrated cement paste (DCP) can recover the original hydration products after rehydration. The mechanical strength of the rehydrated DCP seems to depend on the initial dehydration temperature. Moreover, upon mixing with DCP, an activation effect on fly ash was observed [15].

Upon contact with water, dehydrated phases recover their initial water content. CaO generated from the decomposition of CH and $C\bar{C}$ will react with water to form CH again; the C–S–H gel is also recovered. These rehydration processes are responsible for the buildup of strength, similar to the hydration of cement. Another cause is the hydration of initially unhydrated cement, that was part of the sample before the thermal treatment and that can now hydrate if in contact with water.

Shui et al. [9] reported the compressive strength results obtained from the rehydration of DCP, noticing that the early hydration is very fast – the degree of rehydration after only 1 day reaching 0.7. The degree of rehydration progresses to 0.8, 0.85 and 0.9 in 3, 7 and 28 days respectively, which shows a slower rehydration rate after the initial first day. The explanations for the fast early hydration are the rehydration reactions of the dehydrated reaction products, the difference in the reactants, and the fact that the specific surface of DCP is much higher than the one of cement. As the rehydration progresses, the C–S–H gel will recover its long chains, strengthening the structure.

Table 1
Possible transformations of hardened cement paste samples during thermal treatment at different temperatures [9,14].

Temperature	Transformation
<110 °C	Loss of physically bound water
~450 °C	Dissociation of portlandite
~570 °C	Transformation of quartz
~750 °C	Dissociation of carbonates
~1050 °C	Loss of chemically bound water

2.3. Fresh properties of rehydrated concrete fines pastes

Shui et al. [14] compared the degree of rehydration of DCPs obtained at different maximum temperatures; the evolution of the rehydration was found to be comparable for samples exposed to 400, 600 and 800 °C respectively. It was found that the required water of DCP linearly increases with the increase of the dehydration temperature from 300 °C to 900 °C, which is explained by the advancing of dehydration with temperature. The results show that the water needed to achieve standard consistency of the rehydrated DCP paste increases from 32% for the DCP samples at room temperature up to 68% for the samples treated at 900 °C. The initial and final setting time decreased with the increase of temperature. This would suggest that DCP can be suitable in earth-moist concrete mixes; if used in normal concrete, superplasticizer could be a solution for the higher water demand. The highest compressive strength tests of rehydrated DCP was achieved in the case of DCP treated at 800 °C.

2.4. The use of dehydrated cement paste in new mortar recipes

Shui et al. [14] studied the compressive strength obtained by mortars containing recycled concrete fines (RCF) and the addition of pure cement and fly ash to the mixes. It was concluded that 20% fly ash addition doubles the compressive strength of the mortars. Adding a further 5% Portland cement, the final compressive strength was over four times the one of the mortar with just RCF. The beneficial effect of the fresh cement added can be explained by the quick formation of CH, which in its turn will aid the rehydration of the preheated RCF.

Shui et al. [14] compared the compressive strength obtained using DCP heated at temperatures between 300 and 900 °C to unheated HCP and unhydrated cement. At 3 days curing, the untreated HCP does not develop any new compressive strength, while the DCP heated to 800 °C shows the same strength development as pure cement. The compressive strength increases with the temperature of exposure, from 300 to 800 °C. The sample heated at 900 °C achieves lower strength than the one at 700 °C at early curing times, but reaches almost the values of the sample heated at 800 °C after 28 days.

In this study, real recycled concrete fines are used instead of just cement paste. The main difference in this case is the presence of quartz particles (generated by crushing the concrete aggregates) in the recycled fines. Since this quartz fraction does not contribute to the strength development of the new mixtures, it is important to separate the recycled concrete fractions by silica content and make use of the most beneficial composition.

3. Materials and methods

3.1. The generation of the RCF

Recycled concrete fines generated from laboratory-made concrete were used in this research. This choice was made in order to be able to relate the composition of the concrete fines to the initial concrete one, while also optimizing the crushing method [16–18]. The concrete recipe was designed using an optimized particle packing method [19] and contains 14.5% by mass CEM I 42.5 N, 1.7% limestone and three river aggregate fractions (0–0.125 mm, 0–5.6 mm and a 0.7–8 mm which account for 30.7%, 28.2% and 17.5% by mass, respectively). The composition of all the three aggregate types was measured by XRF and found to be very similar, containing 96–98% SiO_2 and a small amount of iron compounds. A water/cement ratio of 0.5 was used, and the compressive strength of the obtained concrete was tested according to [20]. The mixture attained a compressive strength of 55.15 MPa after 28 days and 60.52 MPa after 91 days. More details regarding the initial concrete mixture can be found in [16–18].

A novel patented [21] crushing method was used, using a jaw crusher specially modified for concrete recycling. The scope of this modified crusher, termed SC1, is to separate concrete into its initial constituents (sand, gravel and cement paste) by using a crushing force that will not damage the aggregates; ordinary crushers are usually used only for the purpose of reducing particle size and so will crush all the component materials randomly. In the case of concrete, this will include crushing through the aggregates as well as between them.

The concrete samples were first pre-crushed in order to simulate the pre-crushing step from practice. Subsequently, the material was crushed two more times. Only particles bigger than 2 mm were re-fed to the crusher [22]. The obtained material was sieved on the 150 μm sieve and the fines, termed RCF (for recycled concrete fines) further used in this study. The choice of maximum particle size was made based on its low silica content, and particle size distribution similar to that of cement, as well as taking into account the yield of the crushing step [16–18].

The PSD of the recycled material is very close to the one of the initial materials used to produce the concrete (Fig. 1), especially in the aggregate size range (over 0.5 mm); this is an indication that the investigated novel crusher indeed separates the initial, clean aggregates from the hydrated cement fines. The deviation at lower particle sizes can be explained by the loss of fines during the consecutive crushing steps. The smart crushing method was found to produce much more recycled concrete fines and cleaner aggregates than a conventional crusher. Moreover, the α-quartz amount of the recycled concrete fines was found to be significantly lower than the one obtained using a commercial jaw crusher. The recovery of the cement paste, in the same particle size range, was improved by ~50%, while the crushed cement paste particles recovery was 7.5 times the one from the conventional jaw crusher [16–18].

The hardened cement paste content of the RCF fraction below 150 μm is approximately 67.4%, the rest of 32.6% being α-quartz. The method for quantifying the α-quartz content of the sample based on DSC measurements is described in detail elsewhere [16–18].

3.2. Thermal treatment program

The TG analysis is used to determine the mass loss of a sample with the variation of temperature. The temperatures at which these mass loss effects occur are associated with the presence of certain compounds within the sample. These results complete the compositional information given by XRF, for instance being able to discern between CaO and $CaCO_3$. Unlike XRD, this technique can also be used to quantitatively, because the percentage of the mass loss can be correlated with the concentration of these components. The DTA curve registers any thermal reaction (exo- or endothermic) which takes place within the sample.

So, both thermogravimetric (TG) and differential thermal analysis (DTA) were performed, together with their first derivatives (DTG and DDTA) on the RCF sample using a Netzsch STA F1. The thermal analysis was performed up to a maximum temperature of 1100 °C, with heating and cooling speeds of 10 °C/min, and a temperature plateau at 1100 °C for 1 h in Al_2O_3 crucibles, to ensure steady state. Fig. 2 shows the TG–DTG analysis results of the recycled concrete fines. The first mass loss effect is visible between 100 °C and 200 °C, due to the liberation of pore water and the liberation of physically bound water from certain hydration products, such as ettringite [10,23]. The second effect happens between 400 °C and 500 °C, due to the dehydration of portlandite [9,11]. The third effect appears at about 570 °C, but only on the DSC curve. The reason is the transformation of quartz [9] which is a crystalline phase change process without mass loss. Around a temperature of 570 °C,

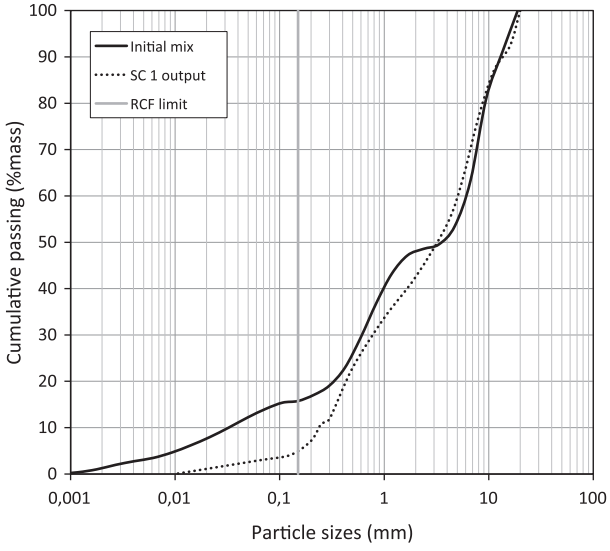

Fig. 1. Particle size distributions of crushed material from the novel crusher SC 1 (SC 1 output) on a logarithmic scale, compared to the initial concrete solids mix (initial mix). The sieving size of 150 μm used for obtaining the RCF fraction is also marked on the graph.

α-quartz undergoes a transformation into β-quartz, which comprises a swell in volume and, therefore, a decrease in density. The densities of α-quartz and β-quartz are 2.65 g/cm^3 and 2.53 g/cm^3, respectively. This transformation is instantaneous and reversible. The quantification of α-quartz in the sample can be done by correlating the area of this peak with the content of α-quartz in known samples [16–18]. The fourth effect of the DSC curve appears between 700 °C and 800 °C: the decomposition of calcium carbonate with loss of CO_2 [9].

Based on the information above, the recycled concrete fines were thermally treated at 500 °C, 800 °C and 1100 °C. These temperatures were chose to be slightly above the temperatures at which the major transformations take place, so that each of the latter can be considered complete.

4. Characterization of the recycled concrete fines

4.1. Chemical composition, PSD and density

The binders used in this research are CEM I 42.5 N (ENCI B.V., Netherlands) and the recycled concrete fines (RCF), as obtained from the crushing (Section 3.1) or thermally treated (Section 3.2). Two commercially available secondary binders were also used: a powder coal fly ash and a ground granulated blast furnace slag. The oxide compositions of all above-mentioned materials are shown in Table 2.

The chemical composition of the RCF can be found in Table 2. It has the estimated CaO content of 33% and the SiO_2 content of 44%, 32% by mass of sample being α-quartz. The loss on ignition is due to the water and CO_2 which can be released through thermal treatment, and its value is in line with the one provided by the TG analysis. The fly ash is a low-lime commercially available fly ash. In the Netherlands, slag-blended cement represents over half of the cement market share [24]. Therefore, a ground granulated blast furnace slag is be employed in this study and its activation by RCF is considered.

In order to verify that a thermal treatment does not affect the PSD of the recycled concrete fines significantly, a grinding test was employed. This step also had the role to decide whether the thermal treatment would be more efficient before the last crushing step (so on 2 mm particles), or on the final RCF-20. The interest was higher for the hardened paste component of the recycled concrete, rather than on the quartz, whose structure after the end of the thermal treatment would not be different. Therefore, samples of hardened cement paste (HCP) with a high water/cement ratio and long mixing time were made, in order to ensure a degree of hydration close to unity. The samples were kept under water for 6 months and then crushed and sieved. The fraction 2–4 mm was selected for the grinding experiments. The samples were then dried in an oven at 110, 400, 600 and 800 °C (and termed HCP-110, HCP-400, HCP-600 and HCP-800, respectively). All these samples, together with a room temperature one (so untreated, termed HCP-20) were ground under the same conditions (grinding time, number of runs, scraping, etc.) and the result analyzed using a Mastersizer 2000 laser diffractometer. The results (cumulative PSD) are shown in Fig. 3.

It can be observed that the room temperature sample possesses the finest PSD. However, no significant difference was found between the samples, except a low tendency to agglomerate for the RCF treated at 110 and 400 °C. The samples treated at higher temperatures (600 and 800 °C) benefited from the volume expansion due to the transformation between α- and β-quartz, and therefore show a PSD very close to the original one. Given the fact that the thermally treated cement paste proved harder to grind than the untreated one (even by a small margin), the thermal treatment was performed on the particles under 150 μm directly, rather than on the 2 mm ones (which would have meant treating also a much larger fraction of the recycled aggregates).

The particle size distributions of the binders were also measured by laser granulometry; the obtained data is shown in Fig. 4. RCF-20 are RCF under 150 μm without thermal treatment (kept at room temperature); RCF-500, RCF-800 and RCF-1100 stand for RCF under 150 μm thermally treated at 500 °C, 800 °C and 1100 °C, respectively. The equivalent particle diameters corresponding to 10%, 50% and 90% passing of all investigated materials ($d_{0.1}$, $d_{0.5}$ and $d_{0.9}$) are presented in Table 3.

Table 2
Chemical composition of the binder materials used in this research: the reference cement (CEM I 42.5 N), the recycled concrete fines with particle sizes under 150 μm (RCF) and the two secondary binders used for comparison (a powder coal fly ash and a ground granulated blast furnace slag commercially available in the Netherlands).

Oxide	CEM I 42.5 N	RCF	Fly ash	Slag
Al_2O_3	5.0	2.3	22.3	12.6
SiO_2	20.0	44.6	55.0	35.0
SO_3	2.2	1.0	1.4	0.1
CaO	63.0	32.8	4.4	39.2
Fe_2O_3	3.0	1.4	8.4	0.4
MgO	1.6	0.7	1.9	8.9
LOI	1.1	17.1	N/A	1.3

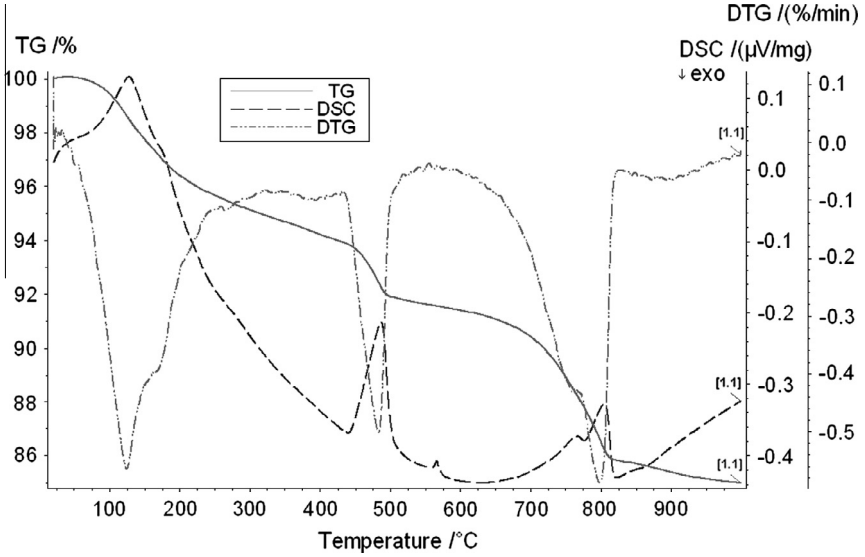

Fig. 2. TG (% mass loss) and DTG (% mass loss/min) curves of the RCF sample, together with its DSC signal curve (μV/mg) for a heating treatment up to 1000 °C.

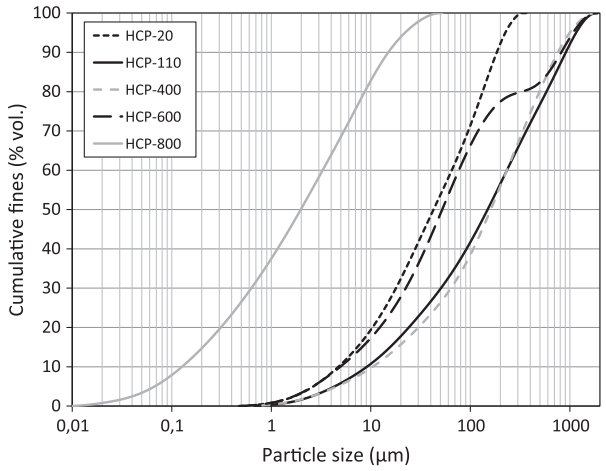

Fig. 3. Particle size distributions of thermally treated (110–800 °C) hardened cement paste samples, all subjected to the same grinding procedure.

It can be seen from Fig. 4 and Table 3 that the slag has the finest particle sizes among all the binders, while the fly ash and the cement have similar particle sizes which are larger than the slag. RCF-20 is made up of even larger particles, which tend to clump together during the thermal treatment (an effect more visible for the RCF-800 and RCF-1100 samples).

Another physical property which was measured before and after each thermal treatment is density. The densities of all RCF samples were measured by an AccuPyc II 1340 He pycnometer. The results are also presented in Table 3. As it was expected, the densities of the RCF increase with the elevated thermal treatment temperature, until 800 °C. This is due to the loss of physically and chemically bound water during the thermal treatment procedure.

4.2. XRD and SEM

X-ray diffraction was performed before and after the thermal treatment of the RCF samples. The samples were analyzed using a Rigaku-Geigerflex spectrometer. The obtained diffractograms of the reference RCF-20, RCF treated at 500 °C (RCF-500) and 800 °C (RCF-800) are illustrated in Fig. 5, where the main crystalline phases are identified and marked. The diffractogram of the gravel

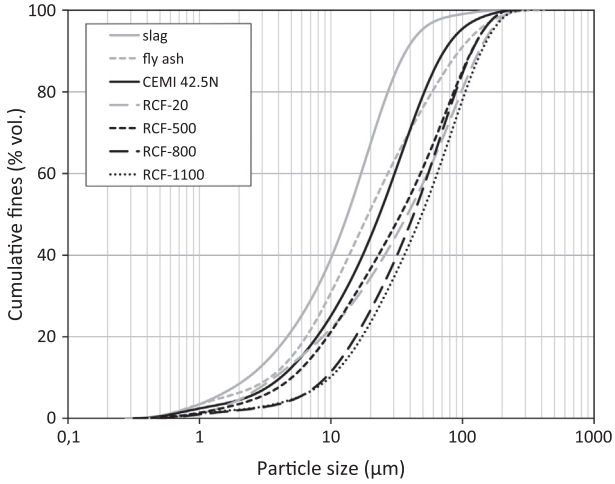

Fig. 4. Particle size distributions of all binder materials used in this research: untreated (RCF-20) and thermally treated recycled concrete fines at different temperatures between 500 and 1100 °C. The cement, fly ash and slag employed in the study are included for comparison.

Table 3
$d_{0.1}$, $d_{0.5}$ and $d_{0.9}$ PSD characteristic parameters and the density measured for the untreated (RCF-20) and thermally treated recycled concrete fines at different temperatures between 500 and 1100 °C. The cement, fly ash and slag employed in the study are included for comparison.

	$d_{0.1}$ (μm)	$d_{0.5}$ (μm)	$d_{0.9}$ (μm)	Density (g/cm^3)
RCF-20	3.7	38.2	133.8	2.52
RCF-500	5.0	33.9	117.2	2.65
RCF-800	9.1	42.5	118.0	2.92
RCF-1100	9.8	49.1	139.6	2.89
CEM I 42.5 N	4.1	23.4	72.6	3.15
Fly ash	3.4	19.2	94.3	2.36
Slag	2.3	13.4	37.1	2.88

used in the initial concrete mix is also added in order to show that the only main phase of this material is α-quartz, and also to serve as comparison for the recycled concrete samples above. The diffractograms of the sand and two types of gravel used in the initial mix are almost identical, which confirms their composition of 96–98% SiO_2 obtained through XRF.

In Fig. 5, the typical reflections associated to α-quartz, C_2S, portlandite, calcite and lime are shown for each of the samples. In the 500 °C-treated sample, the significant differences from the reference RCF-20 due to the reduction of the peaks of portlandite, which correlates with the TG–DSC analysis. Between the temperature of 500 °C and 800 °C, the peaks corresponding to calcite also decrease almost completely. This phenomenon was to be expected, due to the dissociation of calcite at around 750 °C. In the RCF-800 diffractogram, the peaks corresponding to lime are more intense than for RCF-500. The corresponding transformations were listed in Table 1. Portlandite is still present in the 800 °C-treated sample, even though in even lower amount than in the RCF-500, which can be explained by the rehydration of small amounts of the increased CaO content due to atmospheric moisture.

The mineral which is present in all samples and has the highest peak intensities is α-quartz. This can be explained by the presence of crushed silica aggregates in the RCF samples. As explained in Section 3.2, the transformation from α-quartz to β-quartz takes place around 570 °C and is reversible. Therefore, no β-quartz can be detected in the 800 °C-treated RCF, since the XRD is performed after the sample has been cooled down to room temperature.

An interesting observation can be made regarding the detection of a C_2S/C_3S phase in all three RCF diffractograms. This can be attributed to the content of unhydrated cement in the RCF sample, which was to be expected, given the age of the samples is less than 1 year at the time of analysis. A more valuable piece of information is the increase of the C_2S/C_3S peaks intensities in the 800 °C-treated RCF sample, which suggests that the thermal treatment of recycled concrete fines determines the formation of a calcium-rich silicate phase similar to the one found in unhydrated cement.

In order to further observe these transformations visible on the diffractograms, all three RCF samples were also investigated by scanning electron microscopy (SEM). The images are presented in Fig. 6. The samples were analyzed using a high resolution scanning electron microscope (FEI Quanta 600 FEG-SEM) with a Schottky field emitter gun (at a voltage of 2–10 keV) in high vacuum mode. All pictures shown were taken at a magnification of 5000×. Fig. 6a and b show the RCF-20 sample, Fig. 6c and d the RCF-500 sample and Fig. 6e and f the RCF-800 samples.

Hydration products of the recycled concrete fines can be seen in Fig. 6a. Some plate-like formations (portlandite and AFm phases) can be observed. An ettringite needle can be identified, but generally these were not observed in these samples, or observed on the XRD spectra. This can be due to the crushing process, which probably destroyed the fragile ettringite needles. In Fig. 6b, plate-shaped hydration products can be observed more clearly, together

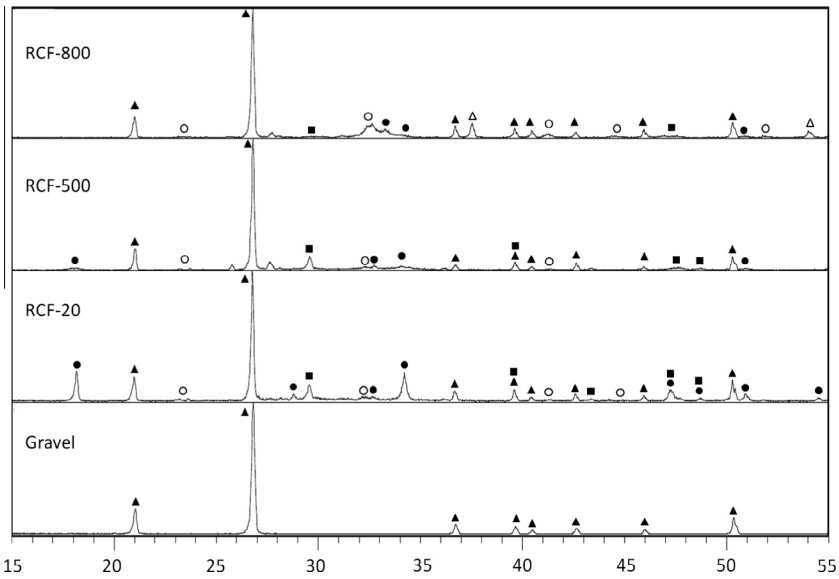

Fig. 5. XRD of reference RCF-20 and thermally treated RCF at 500 °C and 800 °C. A gravel sample used in the initial concrete mix was measured by XRF to contain 98% SiO_2 and is included for comparison. α-Quartz (▲); C_2S (○); portlandite (●); calcite (■); and lime (△).

with a fragment of fractured gypsum, which could not be identified in the XRD analysis, probably due to its low amount in the samples.

Fig. 6c shows a RCF-500 sample, in which the dehydrated cement paste still shows clear plate-like formations. Dehydration cracks are visible in this image, and a fragment of broken calcite can be identified. Fig. 6d further shows plate-shaped hydration products (possibly calcite, which is not yet decomposed at 500 °C) and a piece of fractured quartz (top left corner), generated by the crushing of the aggregates during the pre-crushing stage. This formation is similar to the ones identified in [16–18] and hydration products can be seen on its surface.

Fig. 6e shows cracks on a RCF-800 sample, which can be due to either the dehydration process or to the $\alpha \rightarrow \beta$ quartz transformation, which occurs with a swell in volume. Molten spots can be observed in this image, together with newly-frown formations – small needles which could be C_2S, as indicated by the diffractograms taken of these samples. Fig. 6f also shows local melting, as well as newly formed plates, which can be portlandite, according to the XRD pattern. A feathery structure of decomposed hydration products is visible in the center of the image.

4.3. Calorimetry

All RCF samples were mixed with water and placed in a TAM Air isothermal calorimeter in order to observe and measure their rehydration behavior, which is presented in Fig. 7. Initial tests have shown that there is no significant change recorded between 72 and 168 h (7 days), so all heat generation curves are shown up to 72 h for clarity. The total heat released per gram of binder is presented in Table 4, for a hydration duration of 24 and 72 h. For each sample, the percentage of the cumulative heat relative to the one of the reference is shown in brackets. These values can be compared to the cement content of each sample, also included in Table 4. If they are higher than the cement content, it means that the replacement material contributes to the heat generation. If the two values were the same, the replacement material can be considered inert. A heat ratio lower than the cement content indicates a detrimental effect of the replacement material up to the duration of the rest, 24 or 72 h.

The reference for most of the samples (excluding slag-blended ones as explained below) was a CEM I 42.5 N paste with a w/b ratio of 0.5, obtained as an average of 3 measurements. 10% of the cement was replaced by RCF-20, RCF-500 and RCF-800 respectively, in order to assess the influence of the recycled concrete fines on the cement hydration. Furthermore, samples containing just RCF and water were also analyzed, to see if there is any hydraulic activity present. Due to the large water demand of the recycled concrete fines, the RCF-20 and RCF-500 pastes were mixed with a w/b ratio of 0.7, while RCF-800 needed a w/b of 0.9 to achieve similar flowability before being placed in the calorimeter.

Blended samples containing either fly ash or slag were also tested, in order to test the possibility of using RCF as an activator for pozzolanic binders. Three samples containing 80% CEM I 42.5 N, 10% commercial fly ash and 10% RCF-20, RCF-500 or RCF-800 were measured and the heat release of the fly ash-RCF blends compared to the same cement paste reference. Besides these, four slag-containing samples were also evaluated. Since the most used cement type in the Netherlands is CEM III/B, which has a slag content of 66–80% [26], a sample containing 70% slag and 30% CEM I 42.5 N with a w/b ratio of 0.5 was used as reference. Afterwards, 33% of the cement was in turn replaced by RCF-20, RCF-500 and RCF-800 (for final blends containing 70% slag, 20% CEM I and 10% RCF), while keeping the same water/binder (w/b) ratio.

All samples were mixed externally and then inserted into the measurement slots within minutes of adding the water to the powders. For this reason, the first peak observed on heat flow plots cannot be taken into account. While this peak is partly due to the initial hydration of cement and rehydration of thermally treated RCF, it also includes the disturbance of the system at the introduction of the samples, together with other factors pertaining to the sample preparation. Therefore, this initial high peak will not be included in the computation of the cumulative heat generated by each sample, for which the integration will begin at the inflexion point when the heat flow starts to rise again after the initial drop.

Fig. 7a shows the cumulative heat generated by the RCF-20, RCF-500 and RCF-800, compared to the CEM I curve. For RCF-20, almost no hydration can be detected, this being the lowest of the registered curves. The small heat generation can be attributed to the unhydrated cement that can be contained in the recycled concrete fraction. The RCF-500 sample shows a significantly higher heat generation, due to the rehydration of the thermally treated hydration products (Section 2). Even though, using the same line

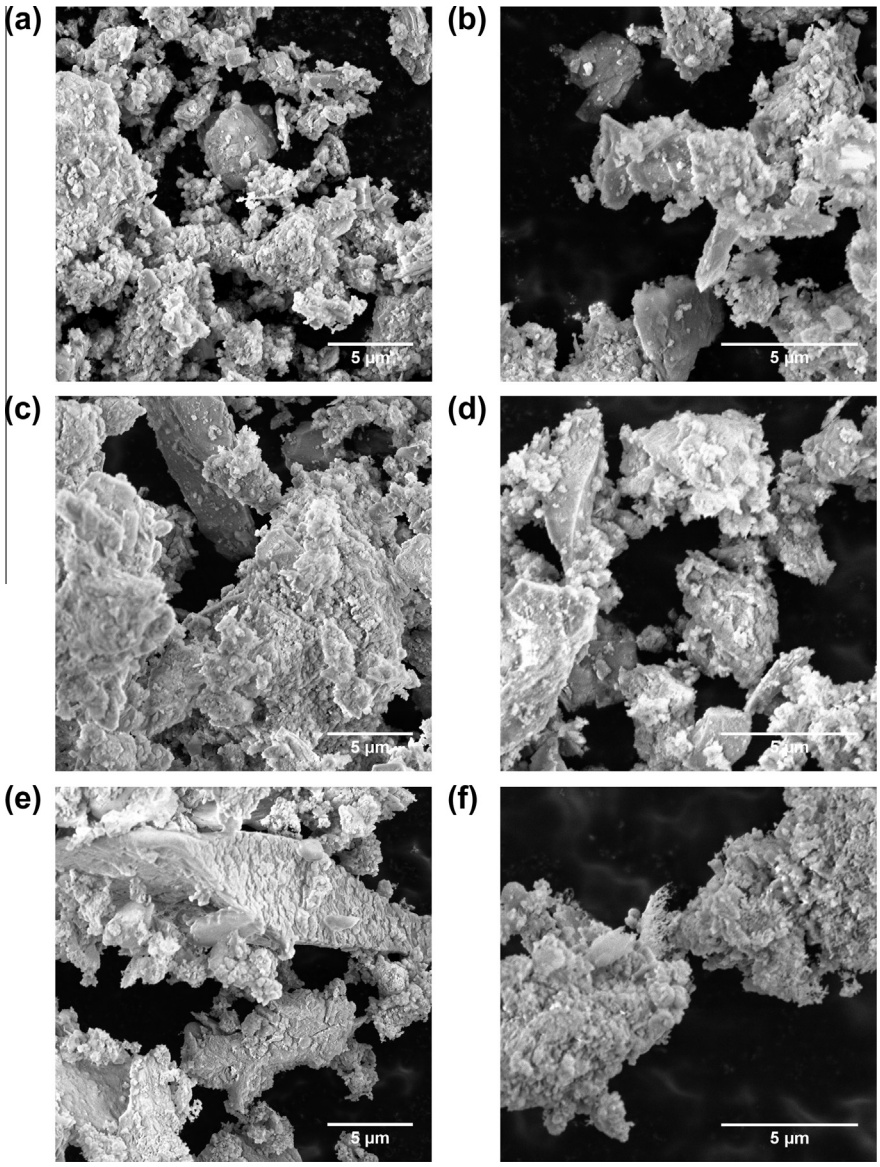

Fig. 6. SEM images of untreated RCF-20 (a and b), 500 °C-treated RCF (c and d) and 800 °C-treated RCF (e and f) at the magnification of 5000×.

of reasoning, the RCF-800 should have the highest heat generation, it has proven to give only slightly higher results than RCF-20. This effect can be attributed to the high water demand of the RCF-800, even though a *w*/*b* ratio of 0.9 was used, compared to a 0.7 ratio for the other two RCF samples. In order to check this hypothesis, Fig. 7b shows only the first 6 h of hydration of the same samples, in terms of heat flow. It can be seen that RCF-800 has a much higher first peak of hydration than RCF-20, RCF-500 or even the pure cement paste. This peak, however, as explained above, cannot be taken into account when computing the cumulative generated heat.

Fig. 7c shows the calorimetric behavior of samples in which 10% of the cement was replaced by untreated or thermally treated RCF. It was found that the addition of RCF-20 does not give promising results. However, RCF-500 and RCF-800 behave in a more promising way, their heat generation after 72 h showing that they do not hinder the hydration of cement after that curing time (Table 4). The RCF-800-containing sample has a better effect than RCF-500, which supports the hypothesis of insufficient water for the hydration of this sample. Three more samples where 20% of the cement was replaced by a mixture of commercial fly ash and the three RCF types in a 1:1 ratio were also studied. The results are shown only in Table 4, as the behavior of all three samples was almost identical. The binding efficiency of all fly-ash – RCF mixes was higher than the replacement level (highest one being 0.94, compared to a cement content level of 0.8, see Table 4), which suggests that they are suitable mixtures for the replacement of cement. This is further studied in Section 5 through mechanical strength tests.

Fig. 7d shows the results obtained by the 4 slag-containing samples. In this case, the mixture containing RCF-500 has proven to be the best one. The poorer performance of the RCF-800 sample can again be explained by the increased water demand of this material. When comparing the results in Table 4, these samples show the most promising effect for the replacement of cement, achieving up to a ratio of 0.87 of the heat generated by the cement at a 0.67 cement content ratio.

5. RCF replacement tests in mortars

5.1. OPC replacement test

Untreated RCF-20, 500 °C-treated RCF (RCF-500) and 800 °C-treated RCF (RCF-800) were used to replace 10%, 20% and 30% by

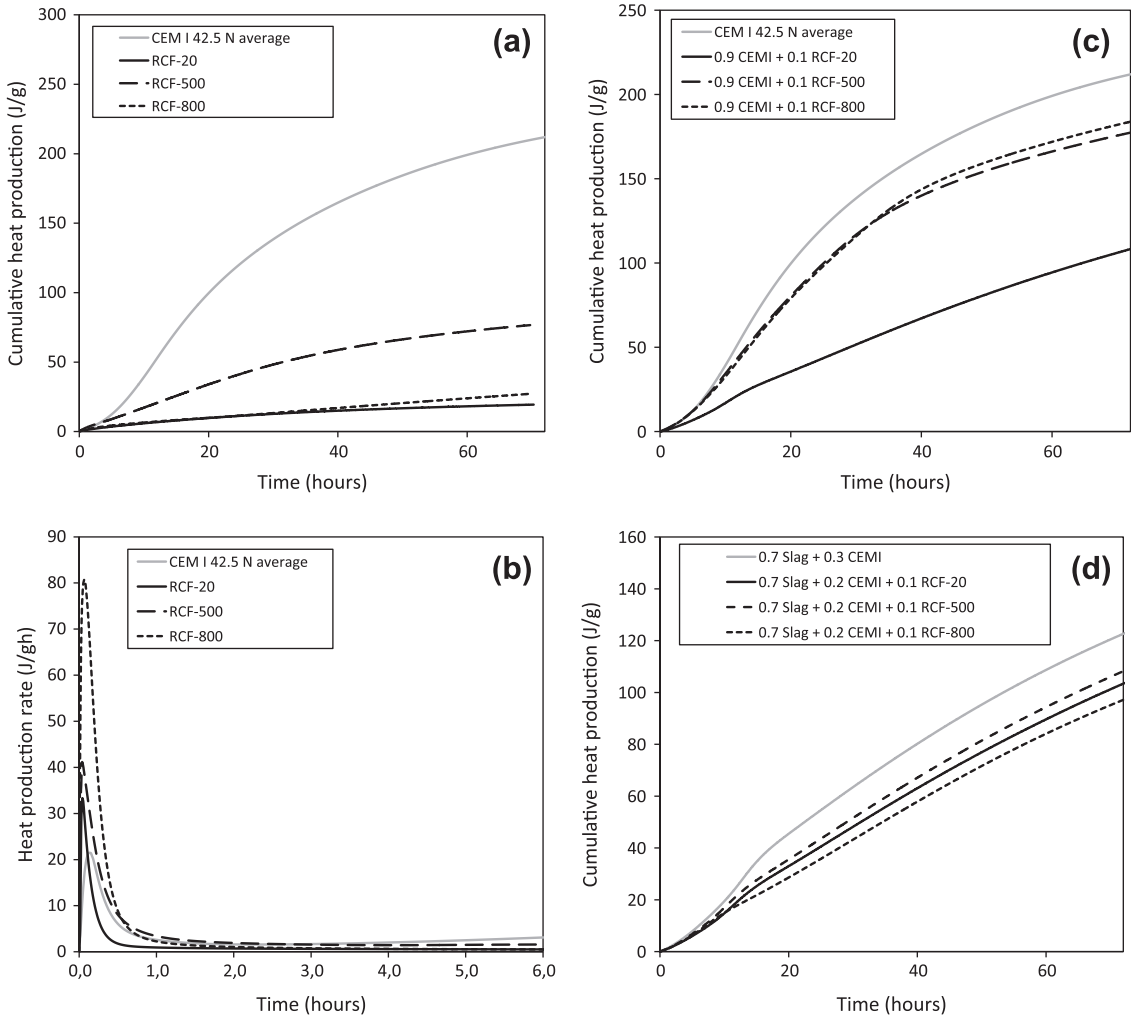

Fig. 7. Calorimetric curves of RCF-20, 500 °C-treated RCF (RCF-500) and 800 °C-treated RCF (RCF-800) in a mix with water (a and b), as 10% cement replacement (c) and as cement replacement in a slag-cement mix (d). Measurements up to 72 h.

mass of cement in the standard mortar recipe. Standard mortar (following [27]) was made as the reference, using CEM I 45.2 N as only binder (1350 g norm sand, 450 g binder, 225 g water). Coal combustion fly ash was used as reference cement replacement. The

Table 4
Total heat released per gram of binder mix for the first 24 and 72 (*70) h of hydration. Mixes shown in bold are used as reference for all following samples. The ratios of cement/total binder in the mix, as well as the ratios between each sample-generated heat and the one of the reference are shown.

Binder	CEM I/binder ratio	Cumulative heat after 24 h (J/g binder) (ratio of reference)	Cumulative heat after 72 h (J/g binder) (ratio of reference)
100% CEM I average	**1**	**107.99**	**209.94**
100% RCF-20	0	10.91 (0.1)	19.39* (0.09)
100% RCF-500	0	38.85 (0.36)	76.63* (0.37)
100% RCF-800	0	10.89 (0.1)	27.07* (0.13)
90% CEM I + 10% RCF-20	0.9	36.78 (0.34)	104.71 (0.50)
90% CEM I + 10% RCF-500	0.9	84.71 (0.78)	174.79 (0.83)
90% CEM I + 10% RCF-800	0.9	84.95 (0.79)	181.53 (0.86)
80% CEM I + 10% fly ash + 10% RCF-20	0.8	93.20 (0.86)	195.79 (0.93)
80% CEM I + 0. 1 fly ash + 10% RCF-500	0.8	97.16 (0.90)	196.81 (0.94)
80% CEM I + 0. 1 fly ash + 10% RCF-800	0.8	90.89 (0.84)	170.46 (0.81)
70% slag + 30% CEM I	–	**47.73**	**119.64**
70% slag + 20% CEM I + 10% RCF-20	0.67	33.78 (0.71)	99.61 (0.83)
70% slag + 20% CEM I + 10% RCF-500	0.67	36.75 (0.77)	104.63 (0.87)
70% slag + 20% CEM I + 10% RCF-800	0.67	28.98 (0.61)	93.28 (0.78)

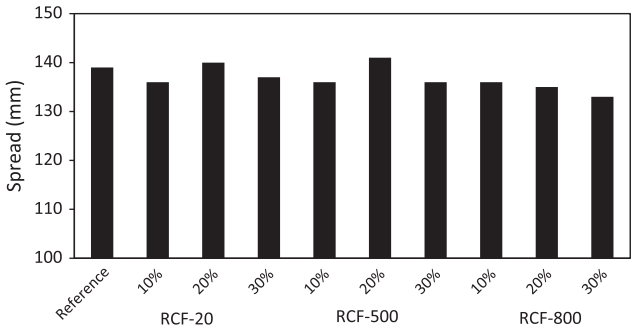

Fig. 8. Final spread of standard fresh mortars (after addition of SP for certain samples, as explained in Section 5): reference (where the binder is CEM I 42.5 N) and 10%, 20% and 30% replacement of the cement by RCF-20, RCF-500 and RCF-800 by mass.

7 and 28 days flexural and compressive strengths were measured in order to quantify the mechanical strength development.

The flowability of the fresh mortar samples was measured following [28]. Both the original and the thermally treated RCFs have a higher water demand than cement. In order to obtain a similar spread as the reference mortar, superplasticizer (Glenium 51, BASF) was applied to the samples in which 20% and 30% of the OPC was replaced by RCF. The 10% replacement samples achieved sufficient flowability without the use of superplasticizer (SP). Fig. 8 shows the spread achieved by the SP-containing mortar samples related to their RCF content. It was expected that the use of RCF would increase the water demand of the mortar samples, decreasing the fresh mortar spread. It was found that additions of 0.12% and 0.24% (by mass of binder) of superplasticizer were needed for the 20% RCF and the 30% RCF replacement mortar samples respectively. RCF-800 displayed the highest water demand, which was to be expected due to its larger free lime content. Moreover, all dehydrated RCF samples will rehydrate very fast upon contact with water, which leads to a higher water demand. The flexural and compressive strength attained by all mortar samples are presented in Fig. 9a–d.

It is observed from Fig. 9a that the 10% RCF-500 containing mortar achieves the lowest flexural strength of its replacement ratio class; fly ash, untreated RCF-20 and RCF-800 obtained very good flexural strength compared to the reference mortar. At a 20% replacement ratio, the highest flexural strength was obtained by the RCF-800 containing mix. Furthermore, for both 10% and 20% replacement ratios, the use of RCF-800 lead to a very similar flexural strength of the sample. Finally, increasing the replacement level to 30% by mass of cement leads to a significant decrease of flexural strength for all investigated mortars mixes; this can be explained by the low flowability achieved by the sample, and therefore the low water availability for the hydration process.

As can be seen from Fig. 9b, RCF-500 continues to have the highest detrimental impact also on the 7 days compressive strength of the mortars. At 10% and 20% replacements, RCF-800 has a higher strength than the rest of the replacement materials, but still lower than the reference. It can be seen that the compressive strengths decrease less than the replacement level, indicating that the RCF brings its own contribution to the strength development. All materials used to substitute 30% of the OPC by mass cause a decrease of the 7 days compressive strength higher than 30%, the coal combustion fly ash leading to the lowest decrease (of 30.8%) compared to the OPC reference.

As can be seen from Fig. 9c, at 28 days the increased replacement ratio no longer decreases the 28 days flexural strength of the mortar samples. For instance, a 30% replacement of OPC by RCF-500 leads to a higher flexural strength (5.84 MPa) than a 20% replacement (5.64 MPa). The same can be observed in the case of

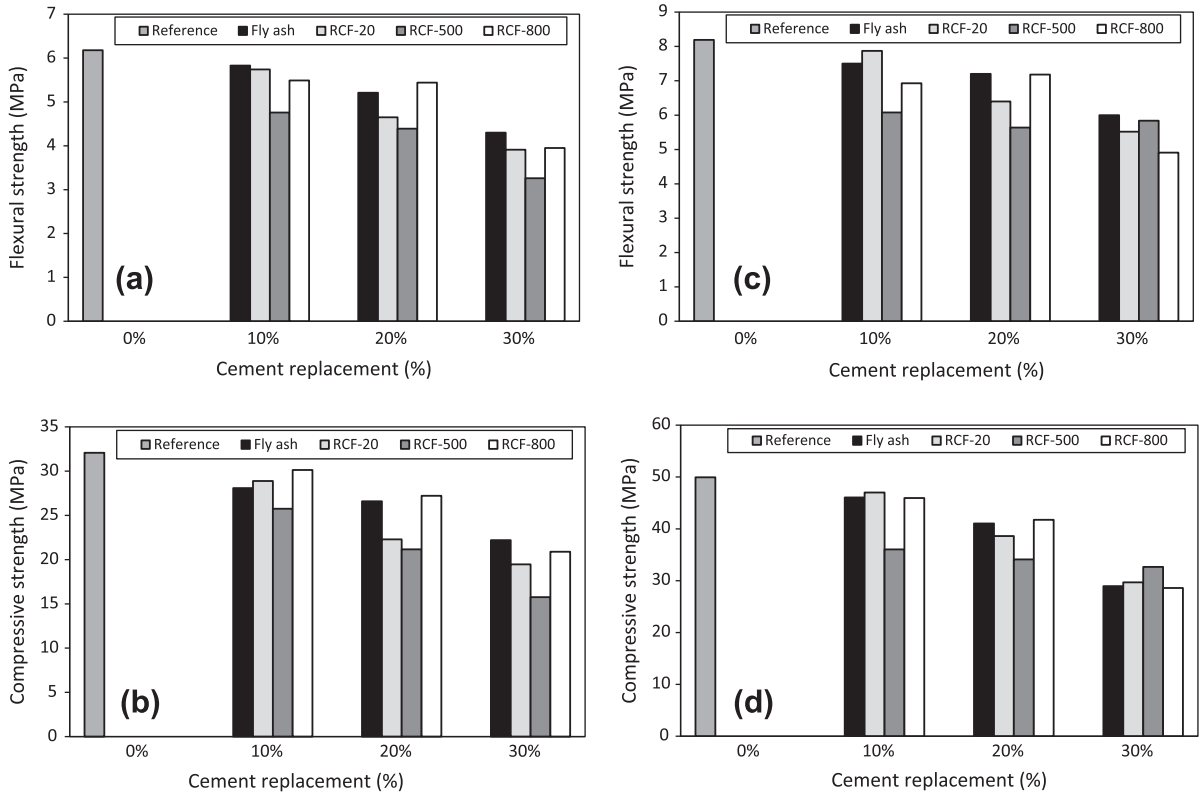

Fig. 9. a. Mechanical properties of standard mortars: reference (where the binder is CEM I 42.5 N) and 10%, 20% and 30% replacement of the cement by fly ash, RCF-20, RCF-500 and RCF-800 by mass. (a) 7 days flexural strength, (b) 7 days compressive strength, (c) 28 days flexural strength, and (d) 28 days compressive strength.

10% and 30% replacement of OPC by RCF-800, which lead to flexural strengths of 6.93 MPa and 7.18 MPa respectively. A 20% replacement of OPC by mass by either coal combustion fly ash or RCF-800 lead to a decrease of less than 20% of the reference sample strength. This indicates that fly ash and RCF-800 can contribute to the 28 days strength development of the mortar samples, which is in line with Shui et al. [14].

At 10% replacement ratio, fly ash, untreated RCF-20 and RCF-800 showed good mechanical performances; the decrease of compressive strength was less than 10% of the reference sample one in all cases and all samples would still qualify as strength class 42.5 following [26]. At 20% replacement ratio, fly ash and RCF-800 performed better than 80% of the strength of the reference mortar, indicating that RCF-800 plays a role in the strength development. Moreover, the samples containing RCF-800 behave very similarly to the ones where coal combustion fly ash was used as secondary binder, for all replacement levels. RCF-500, on the other hand, has the poorest behavior at the 10% and 20% replacement ratios; however, is the best for the 30% replacement ratio.

There are a number of factors which contribute to the obtained results. RCF, either untreated or thermally treated, has a higher water demand than cement. When replacing 10% of OPC by mass, RCF-20 acts mainly as a filler, which can provide nucleation sites for the cement hydration products; at a 20% replacement level, its higher water demand becomes significant, affecting the strength development. RCF-500, which contains dehydrated cement paste including the CaO generated during the thermal treatment, has an even more increased water demand, which will have a greater effect than the rehydration reactions can compensate for.

For comparison purposes, 1100 °C-treated RCF was also used to replace 10% of the cement; however, the attained 28 days compressive strength of this sample proved to be only 36.86 MPa, even lower than the RCF-500. Due to this result (which is in line with [14]), further experiments using RCF-1100 were not performed. An explanation for the poor compressive strength is that at the temperature of 1100 °C, the structures of the hydration products are radically affected by the loss of chemically bound water, so that the initial hydration products cannot be recovered through rehydration.

5.2. Combining thermally treated RCF and fly ash

So far, it has been shown that recycled concrete fines have a binder efficiency comparable to that of powder coal fly ash. Also, Shui et al. [15] has shown that dehydrated cement paste can act as an activator for fly ash. In this research, RCF-800 was combined with coal combustion fly ash as a secondary binder to replace OPC in mortar mixes. It was found that RCF-800 could decrease the fresh mortar flowability. When RCF was used to replace 20% of cement, superplasticizer was needed in order to achieve a good flowability. Fly ash, on the contrary, has the property of increasing the flowability when used in concrete [25]. Moreover, the free lime generated in RCF-800 is believed to activate the pozzolanic properties of fly ash. RCF-800 and fly ash in a 1:1 ratio were used to replace 20% by mass of OPC in standard mortar mixes, thus resulting in the following recipe: 1350 g norm sand, 360 g CEM I 42.5 N, 45 g fly ash, 45 g RCF-800, 225 g water.

The fresh mortar flowability was tested according to [28], the 10% RCF-800 + 10% fly ash mortar sample having a spread of 141 mm (compared 139 mm achieved by the reference sample). Therefore, it can be considered that the use of 10% of fly ash can fully compensate the fresh mortar flowability loss caused by 10% of 800 °C-treated RCF. By using RCF-800 along with fly ash, the flowability of the mix can be maintained while the cement replacement ratio increases.

Mortar recipes made by replacing cement by 20% of RCF-800 and by 20% of fly ash by mass in the standard mortar recipe are also used for comparison; the obtained 7 and 28 days flexural and compressive strengths are shown in Fig. 10a and b. As it can be seen in Fig. 10a, the sample in which both RCF and fly ash are used reaches the lowest 7 days flexural strength of the group (reduced by 36.7% from the reference). However, the same sample attained a 28 days flexural strength of 7.19 MPa, which is only 12.2% lower than the reference, which suggests that the strength development of the combination of fly ash and RCF-800 continues over longer curing periods.

It is illustrated in Fig. 10b that all three 20% cement replacement samples achieve very close 28 days compressive strengths. The sample containing both fly ash and RCF-800 has a compressive strength development which mirrors its slow flexural strength development.

The following conclusions can be drawn based on the experimental results: fly ash is able to compensate the fresh mortar flowability loss caused by 800 °C-treated RCF. Using both RCF-800 and coal combustion fly ash in a 1:1 ratio leads to slow strength development, but its 28 days mechanical properties are encouraging.

5.3. Slag cement replacement test

In the Netherlands, CEM III/B (which contains 66–80% ground granulated blast furnace slag [26]) represents over half of the binder market [24]. In order to quantify the influence of RCF on the hydration of slag-blended cement, mortar samples containing 70% of slag mixed with 30% of cement as binder were made as reference. RCF, both untreated and thermally treated, were used to replace 33% of the cement in the slag-cement blend, thus the recipes using a binder combination of 70% slag, 20% CEM I and 10% RCF.

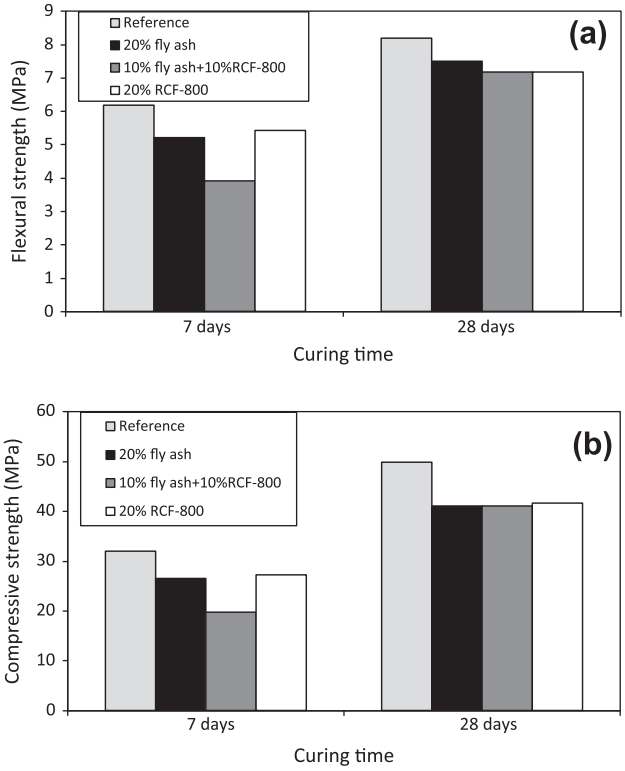

Fig. 10. (a) 7 days and 28 days flexural strength of the reference, 10% 800 °C-treated RCF + 10% fly ash, 20% 800 °C-treated RCF and 20% fly ash replacement mortars. (b) 7 days and 28 days compressive strength of the reference, 10% 800 °C-treated RCF + 10% fly ash, 20% 800 °C-treated RCF and 20% fly ash replacement mortars.

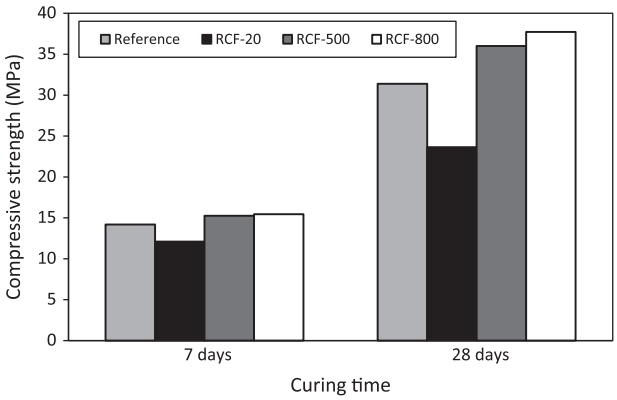

Fig. 11. 7 days and 28 days compressive strength of slag-blended cement mortars, containing 70% slag + 20% CEM I + 10% RCF as binder.

The water/binder ratio was kept at 0.5. Fig. 11 presents the 7 and 28 days compressive strength of these mortars.

It can be seen from Fig. 11 that the untreated RCF-20 containing mix achieves the lowest compressive strength after both 7 and 28 days of curing. Both RCF-500 and RCF-800 increase the 7 and 28 days compressive strengths by 7.5% and 14.7% and respectively 8.8% and 20.1%, probably due to their increased free lime content, as well as the rehydration of their initial hydration products.

5.4. Comparison between expected and achieved binding ability of RCFs

Table 5 compares the 7 and 28-days compressive strengths of all the mortars detailed in Section 5 to the one of the reference mortars. Just as in the case of the calorimetry results (Table 4), a ratio between the compressive strength of each sample containing RCF and its reference mortar compressive strength is computed, in order to be related to the cement ratio of the sample. It can be observed that the use of 10% RCF-20, 10% RCF-800, 20% RCF-800 and 10% RCF-800 + 10% fly ash lead to a higher compressive strength than if an inert material would have been used as cement replacement. An interesting observation is that the compressive strength ratio after 28 days is in some cases lower than the one after 7 days, especially in the case of the thermally-treated fines, as well as for the higher cement replacement level of 30%. This suggests that the beneficial effect of the additions manifests itself in the early hydration stages. The only samples that achieves a higher compressive strength than if using an inert filler are those containing slag and thermally treated recycled concrete fines. Both RCF-500 and RCF-800 prove to be able to activate the slag in the mixture to a certain degree, which can be explained by their higher content of CaO which will regenerate portlandite for the slag hydration upon contact with water. Moreover, in the case of RCF-800, this effect is even more pronounced after 28 days than after 7 days, which is consistent with the slower hydration of the slag. This effect can also be observed for the sample containing 10% RCF-800 + 10% fly ash, for which a similar explanation can be envisaged.

These 4 samples containing either fly ash or slag and RCF, as well as the ones containing 90% CEM I and 10% RCF were also analyzed using isothermal calorimetry (Table 4). It can be said almost unanimously for these samples that the compressive strength achieved was higher than indicated by the calorimetric results. This suggests that the recycled concrete fines have not only a role in generating compressive strength by their rehydration or hydration of residual unhydrated cement, but also by providing a filler effect in mortar mixes, as well as probably acting as nucleation sites for the further hydration of the cement component. Both these effects cannot be indicated by calorimetry, but are probable due to the increased compressive strength achieved, especially for the containing 90% CEM I + 10% RCF samples, for which it was shown that the main beneficial effect of RCF is manifested in the first hours of hydration. For the slag- and fly-ash- containing samples, it would be interesting to also follow the strength development over longer curing times. This will be done in a future study, together with optimizing the mix parameters in order to maximize the beneficial effect of RCF. At longer curing times, also the possible contribution of the newly formed calcium silicate phase indicated on the XRD pattern of RCF-800 needs attention.

6. Conclusions and discussions

The main objective of this research was to use recycled concrete fines (RCF) generated through a novel crushing method to replace part of the cement in new mortar mixes. A thermal treatment method was employed to test its activation effect on the recycled fines. The characterization of the thermally-treated RCF suggested that a calcium silicate phase similar to the ones in cement is

Table 5
Compressive strength of all mortar samples after 7 and 28 days. Mixes shown in bold are used as reference for all following samples. The ratios of cement/total binder in the mix, as well as the ratios between each sample strength and the one of the reference are shown.

Binder	CEM I/binder ratio	Compressive strength 7 days (MPa) (ratio of reference)	Compressive strength 28 days (MPa) (ratio of reference)
100% CEM I	**–**	**32.07**	**49.94**
90% CEM I + 10% fly ash	0.9	28.09 (0.88)	46.06 (0.92)
90% CEM I + 10% RCF-20	0.9	28.89 (0.90)	47.00 (0.94)
90% CEM I + 10% RCF-500	0.9	25.75 (0.80)	36.03 (0.72)
90% CEM I + 10% RCF-800	0.9	30.13 (0.94)	45.94 (0.92)
80% CEM I + 20% fly ash	0.8	26.6 (0.83)	41.03 (0.82)
80% CEM I + 20% RCF-20	0.8	22.29 (0.70)	38.62 (0.77)
80% CEM I + 20% RCF-500	0.8	21.16 (0.66)	34.1 (0.68)
80% CEM I + 20% RCF-800	0.8	27.21 (0.85)	41.74 (0.84)
70% CEM I + 30% fly ash	0.7	22.20 (0.69)	28.95 (0.58)
70% CEM I + 30% RCF-20	0.7	19.46 (0.61)	29.69 (0.59)
70% CEM I + 30% RCF-500	0.7	15.76 (0.49)	32.66 (0.65)
70% CEM I + 30% RCF-800	0.7	20.89 (0.65)	28.6 (0.57)
10% RCF-800 + 10% fly ash	0.8	19.86 (0.62)	41.14 (0.82)
70% slag + 30% CEM I	–	**14.19**	**31.39**
70% slag + 20% CEM I + 10% RCF-20	0.67	12.10 (0.85)	23.64 (0.75)
70% slag + 20% CEM I + 10% RCF-500	0.67	15.26 (1.26)	36.01 (1.15)
70% slag + 20% CEM I + 10% RCF-800	0.67	15.45 (1.01)	37.72 (1.20)

formed during the treatment at 800 °C, which should be further investigated. It was found that the rehydration of the thermally treated concrete fines is a rapid process, occurring in the first hour after contact with water. Also, the 800 °C-treated RCF required a higher water/binder ratio to achieve full rehydration. The calorimetric measurements indicate that mixing RCF and fly ash or slag is the most promising way of reuse for both the untreated and thermally treated concrete fines.

It was demonstrated in this study that untreated RCF-20 and 800 °C-treated RCF can be used to replace up to 20% of the cement in standard mortar samples without a significant loss of strength. The samples with 10% of the CEM I 42.5 N cement replaced by untreated RCF-20 or 800 °C-treated RCF still meet the criteria of strength class 42.5 as described in [26]. The mechanical strength of RCF-800-containing mortars was also compared to a class F fly ash- containing mortar. It was found that 800 °C-treated RCF had mechanical performances equivalent to fly ash. 500 °C-treated RCF-containing mortars showed a more significant strength loss at a 20% cement replacement level; the same effect was observed when the replacement of 30% of cement was attempted by all considered secondary binders.

RCF samples treated at both 500 °C and 800 °C showed an activation effect on ground granulated blast furnace slag. It was found that the replacement of CEM I by 10% of 500 °C-treated RCF and 800°C-treated RCF can increase the 28 days compressive strength of the slag-cement blend by 14.7% and 20.1% respectively, which can be attributed to the higher lime content of these samples.

Most of the mortar samples containing RCFs were found to have a higher compressive strength than their cement content, which suggests that the addition of recycled concrete fines also contributes to the development of mechanical properties. This can be due to the rehydration of the thermally treated fines, but also to the filler effect of all RCFs, as well as their contribution by providing nucleation sites for the hydration of cement. Further studies will focus on this possibility, together with optimizing the mix in terms of particle size and water/binder ratio, and the study of longer term strength development, among other topics.

Acknowledgements

The authors wish to express their gratitude to Schenk Concrete Consultancy and Theo Pouw Groep for the support in this project, as well as to the following sponsors of the Building Materials research group at TU Eindhoven: Rijkswaterstaat Centre for Infrastructure, Graniet-Import Benelux, Kijlstra Betonmortel, Struyk Verwo, Attero, Enci, Provincie Overijssel, Rijkswaterstaat Directie Zeeland, Van Gansewinkel Minerals, BTE, Alvon Bouwsystemen, V.d. Bosch Beton, Selor, Twee "R" Recycling, GMB, Geochem Research, Icopal, BN International, APP All Remove, Consensor, Eltomation, Knauf Gips, Hess ACC Systems, Kronos and Joma (in chronological order of joining) for making this research possible, to Dr. Dipl.-Ing. G. Hüsken for designing and testing the concrete mix, to Dipl.-Min. C. Straub for his contribution to the analysis part, to Mr. P. Cappon for the helpful assistance in the laboratory and to MSc. P. Spiesz and Dipl. Eng. D. Florea for their help and advice on this manuscript.

References

[1] CEMBUREAU. World cement production 2010. Brussels: The European Cement Association; 2011.
[2] Meyer C. The greening of the concrete industry. Cem Concr Compos 2009;31:601–5.
[3] CSI. Cement sustainability initiative – recycling concrete. Geneva: World Business Council for Sustainable Development; 2011.
[4] Tam VW. Comparing the implementation of concrete recycling in the Australian and Japanese construction industries. J Clean Prod 2009;17:688–702.
[5] Oikonomou ND. Recycled concrete aggregates. Cem Concr Compos 2005;27:315–8.
[6] CSI. Cement sustaibability initiative – recycling concrete. Geneva: World Business Council for Sustainable Development; 2009.
[7] Husain A, Assas MM. Utilization of demolished concrete waste for new construction. World Acad Sci Eng Technol 2013;73:605–10.
[8] Li X. Recycling and reuse of waste concrete in China: Part I. Material behaviour of recycled aggregates concrete. Resour Conserv Recy 2008;53:36–44.
[9] Shui Z, Dongxing X, Huiwen W, Beibei C. Rehydration reactivity of recycled mortar from concrete waste experienced to thermal treatment. Constr Build Mater 2008;22:1723–9.
[10] Castello M, Alonso C, Andrade C, Turrillas X, Campo J. Composition and microstructural changes of cement pastes upon heating, as studied by neutron diffraction. Cem Concr Res 2004;34:1611–44.
[11] Alonso C, Fernandes L. Dehydration and rehydration processes of cement paste exposed to high temperature environments. J Mater Sci 2004;39:3015–24.
[12] Handoo S, Agarwal S, Agarwal S. Physicochemical, mineralogical, and morphological characteristics of concrete exposed to elevated temperatures. Cem Concr Res 2002;32:1009–18.
[13] Tayyib A. The effect of thermal cycling on the durability of concrete made from local materials in the Arabian Gulf countries. Cem Concr Res 1989;19:131–42.
[14] Shui Z, Xuan D, Chen W, Yu R, Zhang R. Cementitious characteristics of hydrated cement paste subjected to various dehydration temperatures. Constr Build Mater 2009;23:531–7.
[15] Shui Z, Yu R, Jun D. Activation of fly ash with dehydrated cement paste. ACI Mater J 2011;108:108–12.
[16] Florea MVA, Brouwers HJH. Recycled concrete fines and aggregates: the composition of various size fractions related to crushing history. In: Proceedings of the international conference on building materials (IBAUSIL); 2012. p. 1034–41.
[17] Florea MVA, Brouwers HJH. Properties of various size fractions of crushed concrete related to process conditions and re-use. Cem Concr Res 2013;52:11–21.
[18] Florea MVA, Brouwers HJH. The influence of crushing method on recycled concrete properties. In: Proceedings of the international conference on advances in cement and concrete technology in Africa, Johannesburg (South Africa); 2013. p. 1041–50.
[19] Hüsken G, Brouwers HJH. Earth-moist concrete: application of a new mix design concept. Cem Concr Res 2009;38:1246–59 [Erratum, ibid 39, 832].
[20] EN 12390-3: 2009. Testing hardened concrete. Compressive strength of test specimens; 2009.
[21] Schenk KJ. WO 2011/142663; 2011.
[22] Ning Z. Thermal treatment of recycled concrete fines. Eindhoven University of Technology; 2012.
[23] Alarcon-Ruiz L, Platret G, Massieu E. The use of thermal analysis in assessing the effect of temperature on a cement paste. Cem Concr Res 2005;35:609–13.
[24] Chen W. Hydration of slag cement – theory, modeling and application. University of Twente; 2006.
[25] Illston J, Domone P. Construction materials – their nature and behaviour. London: Spon Press; 2001.
[26] EN 197-1. Cement – Part 1: Composition, specifications and conformity criteria for common cements; 2000.
[27] EN 196-1:2005. Methods of testing cement. Determination of strength; 2005.
[28] EN 1015-3:1999. Methods of test for mortar for masonry. Determination of consistence of fresh mortar (by flow table); 1999.